ChemPubSoc Europe

DOI: 10.1002/chem.201903949

CHEMISTRY A European Journal Full Paper

Polymer Chemistry |*Hot Paper*|

Undiscovered Potential: Ge Catalysts for Lactide Polymerization

Ruth D. Rittinghaus,[a] Jakub Tremmel,[b] Ales Růžička,[b] Christian Conrads,[a] Pascal Albrecht,[a] Alexander Hoffmann,[a] Agnieszka N. Ksiazkiewicz,[c] Andrij Pich,[c, d, e] Roman Jambor,*[b] and Sonja Herres-Pawlis*[a]

Abstract: Polylactide (PLA) is a high potential bioplastic that can replace oil-based plastics in a number of applications. To date, in spite of its known toxicity, a tin catalyst is used on industrial scale which should be replaced by a benign catalyst in the long run. Germanium is known to be unharmful while having similar properties as tin. Only few germylene catalysts are known so far and none has shown the potential for industrial application. We herein present Ge complexes in combination with zinc and copper, which show amazingly high polymerization activities for lactide in bulk at 150 °C. By systematical variation of the complex structure, proven by single-crystal XRD and DFT calculations, structure–property relationships are found regarding the polymerization activity. Even in the presence of zinc and copper, germanium acts as the active site for polymerizing probably through the coordination–insertion mechanism to high molar mass polymers.

Introduction

Milestone innovations in the production and application of plastic as a manifold material in the last decades led to a steadily rising demand. However, it came along with massive environmental problems.[1] One way out is the use of biodegradable plastics.[2] A prominent example for a biocompatible polymer, which has potential to replace conventional polymers in many applications, is polylactide (PLA).[3] The monomer, lactide, is obtained from biomass and the polymer itself is biodegradable.[4] Next to medical applications for example, as self-dissolving threads, PLA is used as 3D printing material and for single-use items like cups or lids.[5] With a production capacity of PLA in 2016 of 220 Mt, PLA is the most widely used biodegradable bioplastic and is predicted to triple its production capacity until 2020.[6] PLA is most efficiently produced by a ring-opening polymerization (ROP) of lactide with a catalyst and, if necessary, a coinitiator. Different mechanisms are known for the ROP of lactide; however, the best control is reached when following the coordination–insertion mechanism.[7] With the predicted production capacity growth rate of PLA it is peculiar, that the industrially used catalyst for the polymerization contains tin, which has toxic effects when introduced to the biological cycle.[8] A variety of effective catalysts are already known for the polymerization of lactide.[9] However, in spite of intensive research efforts only few catalysts could stand the high criteria necessary to be fulfilled for industrial application.[10] An alternative catalyst should be able to polymerize under solvent-free conditions with small catalyst loadings and must be robust towards air, moisture and small amounts of impurities (e.g. water, lactic acid) in technical grade lactide.[9,11] Iron and zinc are prominent metal candidates for an alternative, biocompatible industrial catalyst and great improvements have been achieved with robust catalysts recently.[10a–c,12] A metal, which has potential due to its similar properties to tin, but no harmful effects, is germanium.[13] Surprisingly, only very few examples of Ge catalysts for the ROP of lactide have been reported. Germanium was first tested for the polymerization of lactones in 2002 by Kricheldorf et al., with the finding that the alkoxides are less active than the analogous tin compounds.[14] An enhanced version of the catalysts was tested in solution and bulk by Albertsson et al. who showed that the complexes polymerize in a controlled manner following pseudo-first-order

[a] *R. D. Rittinghaus, C. Conrads, P. Albrecht, Dr. A. Hoffmann, Prof. Dr. S. Herres-Pawlis*
Institute of Inorganic Chemistry, RWTH Aachen University
Landoltweg 1, 52074 Aachen (Germany)
E-mail: sonja.herres-pawlis@ac.rwth-aachen.de

[b] *J. Tremmel, Prof. Dr. A. Růžička, Prof. Dr. R. Jambor*
Department of General and Inorganic Chemistry
Faculty of Chemical Technology, University of Pardubice
53210 Pardubice (Czech Republic)
E-mail: roman.jambor@upce.cz

[c] *A. N. Ksiazkiewicz, Prof. Dr. A. Pich*
Institute of Technical and Macromolecular Chemistry
RWTH Aachen University, Worringerweg 2, 52074 Aachen (Germany)

[d] *Prof. Dr. A. Pich*
DWI—Leibniz Institute for Interactive Materials e.V.
Forckenbeckstr. 50, 52074 Aachen (Germany)

[e] *Prof. Dr. A. Pich*
Aachen Maastricht Institute for Biobased Materials (AMIBM)
Maastricht University, Brightlands Chemelot Campus
Urmonderbaan 22, 6167 RD Geleen (The Netherlands)

Supporting information and the ORCID identification number(s) for the author(s) of this article can be found under: https://doi.org/10.1002/chem.201903949.

kinetics producing polymers with low polydispersity.[15] The first single-site germanium catalyst was published by Davidson et al. and showed as the first catalyst ever a highly heterotactic polymerization behavior for racemic lactide in bulk. With 70% conversion after 24 h at 130 °C and a monomer to initiator (*M*/*I*) ratio of 600:1, the catalyst came closer to industrial relevance.[16] Very different reaction conditions were applied for catalysts published by Thomas et al.: The germanium alkoxide complexes polymerized 400 equivalents of sublimed lactide at 1 mol L^{-1} in THF at 20 °C in 10 min which is in the same activity range with other catalysts for polymerization in solution.[9d,17] Similar conditions were used by Sarazin et al. to compare the polymerization activity of germylene, stannylene, and plumbylene complexes to find that the first have the lowest activity.[18] Taking the unacceptable toxicity of the latter two compounds into account, this finding appears less relevant. The latest update on germanium catalysts was published in 2018 by Kricheldorf et al. who use germylene compounds for ring-expansion polymerization of lactide with rather low activities and small molar masses.[19] These examples show, that the potential of germylene compounds as less toxic alternatives to tin catalysts were recognized by the scientific community, but to date no complex was found to hold the expectations.

In addition to Ge-only complexes, it was already shown that germylenes may act as ancillary ligands in Group 11 metal complexes (Figure 1 **I**–**VIII**).[20] The efficient Ge→M (M = Cu, Ag) donation allows synthesis of germylene-metal cations (Figure 1 X–**XI**),[21] which indicates the possible tuning of the Ge^{II} electrophilic character within the complexes. Interestingly, analogous complexes with $ZnCl_2$ are quite rare (Figure 1, **IX**)[22] although Zn complexes are useful catalysts for the ROP of cyclic esters.[9a,d,10b,23] Therefore, we set out to combine the germylenes as ancillary ligands for $ZnCl_2$ to prepare a new type of catalysts for the ROP of lactide.

Recently, we have shown that the organogermanium(II) chloride L(Cl)Ge acts as ancillary ligand for $M(CO)_5$ fragments.[24] The ligand L (L = 2-Et_2NCH_2-4,6-tBu_2-C_6H_2) provided the stabilization of the Ge^{II} atom by N→Ge coordination and an efficient steric protection due to the presence of a *t*Bu group and the complexes {(LGeX)$M(CO)_5$} (M = Cr, W, X = Cl, H) with different polarity of the Ge*X* fragment were prepared. In the present study, we focus on the complexation of $ZnCl_2$ and CuX halides (X = Cl and I) by L(Cl)Ge. The resulting complexes with different electrophilic character of the Ge^{II} atom have been tested as new type catalysts in the ROP of lactide and found to excel all Ge systems reported so far.

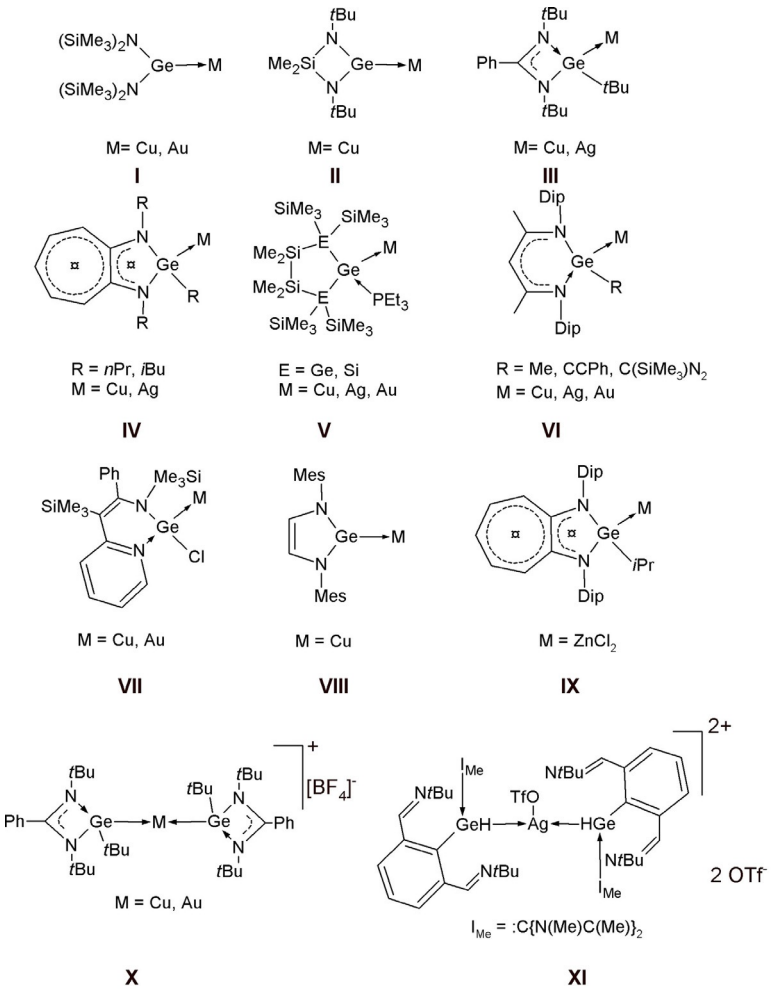

Figure 1. Types of germylenes used as ligands in Group 11 and 12 metal complexes.

Results and Discussion

Complex synthesis and characterization

The starting compound L(Cl)Ge (**1**) was prepared according to the literature procedure.[24–25] Subsequent treatment of **1** with 1 equiv. of the halide salts $ZnCl_2$, CuCl, and $(CuI)_4{\cdot}(SMe_2)_3$ provided the dimeric complexes {[L(Cl)Ge]ZnCl(μ-Cl)}$_2$ (**2**), {[L(Cl)Ge]Cu(μ-Cl)}$_2$ (**3**), and {[L(Cl)Ge]Cu(μ-I)}$_2$ (**4**) (Scheme 1), which were characterized by NMR spectroscopy as well as X-ray diffraction (**2** and **3**). The molecular structures of complexes **2** and **3** are shown in Figure 2 while selected bond lengths and angles are given in Table 1 (the crystallographic parameters are given in Table S1 in the Supporting Information). The ^{1}H NMR spectra of **2**–**4** ($CDCl_3$) are consistent with the molecular structures found for **2** and **3**. The CH_2N protons of the ligand resonate as AB spin systems ranging from δ = 4.19 (**4**) to 4.26 (**2**) ppm. The aromatic C*H* protons of the ligand resonate as two signals in the range of δ = 7.00 to 7.43 ppm.

The presence of M(μ-X) bridges in dimeric complexes suggest that analogous monomeric complexes can be obtained with a higher ratio of ligand and, therefore, the reaction of **2**–**4**

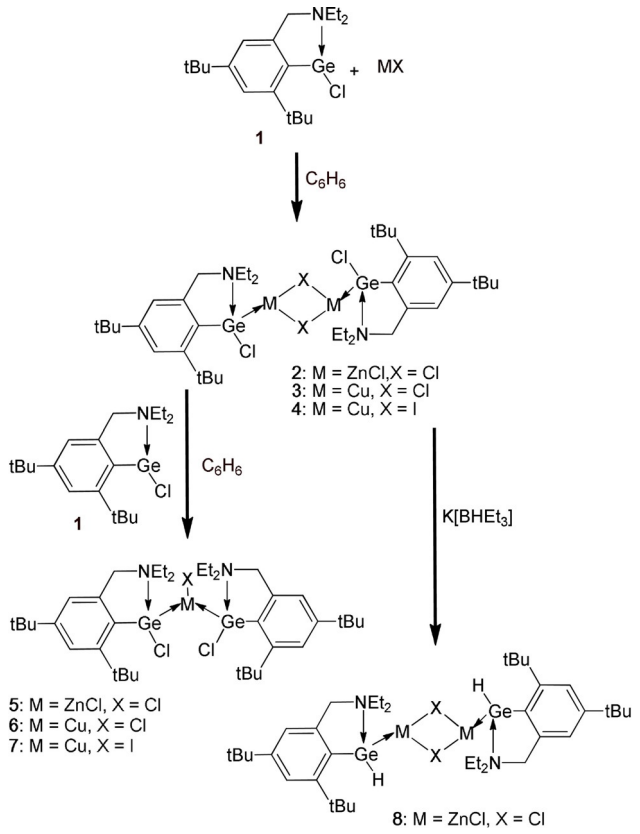

Scheme 1. Synthesis of Complexes **2**–**8**.

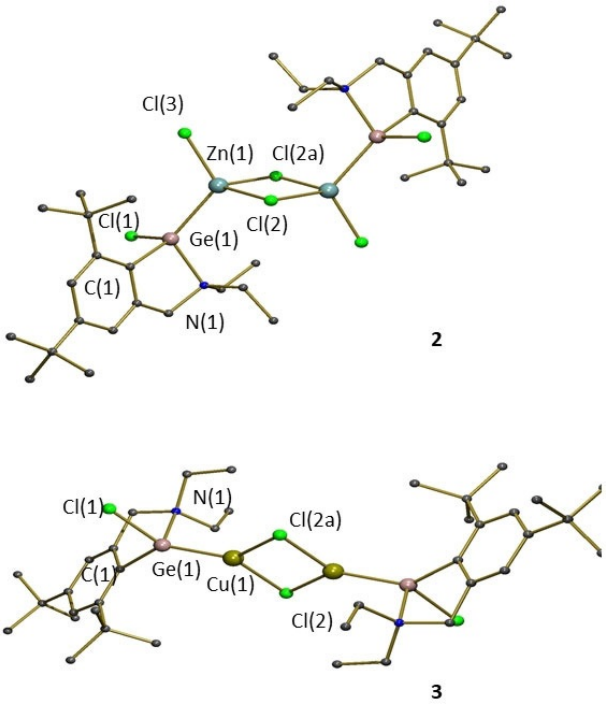

Figure 2. Molecular structures of compounds **2** and **3**. Hydrogen atoms and solvate molecules are omitted for clarity.

with another equivalent of **1** was tested. These reactions provided the monomeric complexes $[L(Cl)Ge]_2ZnCl_2$ (**5**), $[L(Cl)Ge]_2CuCl$ (**6**), and $[L(Cl)Ge]_2CuI$ (**7**) (Scheme 1), which were characterized by NMR spectroscopy and X-ray diffraction analysis (**7**). Complexes **5**–**7** may also be prepared by direct reaction of two equivalents of **1** with the halide salts $ZnCl_2$, CuCl, and $(CuI)_4{\cdot}(SMe_2)_3$ (see the Experimental Section). The molecular structure of complex **7** is shown in Figure 3, while selected

Table 1. Selected bond lengths [Å] and angles [°] in **2**, **3** and **7** determined by XRD and DFT calculations.

	2 M = Zn, X = Cl(2)		**3** M = Cu, X = Cl(2)		**7** M = Cu, X = I(1)	
	XRD	DFT[a]	XRD	DFT[a]	XRD	DFT[a]
M(1)–X	2.3454(9)	2.407	2.2710(8)	2.389	2.5051(13)	2.625
Ge(1)–M(1)	2.4615(5)	2.559	2.2700(5)	2.441	2.3429(8)	2.514
Ge(1)–Cl(1)	2.2050(8)	2.215	2.2410(6)	2.241	2.2562(17)	2.260
Ge(1)–N(1)	2.047(2)	2.079	2.085(2)	2.110	2.101(4)	2.105
Cl(2a)-M(1)-X	95.17(3)	93.70	103.89(3)	104.39	–	–
Ge(1)-M(1)-X	115.76(2)	113.89	136.08(2)	133.34	116.41(3)	119.19
M(1)-Ge(1)-C(1)	130.33(6)	127.51	135.75(6)	131.45	131.54(18)	131.83
M(1)-Ge(1)-Cl(1)	113.67(3)	119.66	119.29(2)	122.95	118.11(6)	121.80

[a] M06-2X/def2-TZVP.

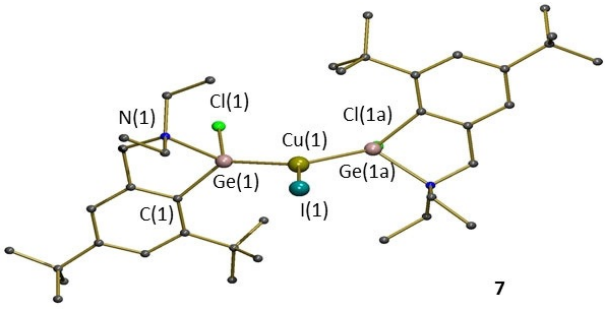

Figure 3. Molecular structure of **7**. Hydrogen atoms and solvate molecules are omitted for clarity.

bond lengths and angles are given in Table 1 (the crystallographic parameters are given in Table S1 in the Supporting Information). The ^{1}H NMR spectra of **5**–**7** ($CDCl_3$) are consistent with the molecular structures found for **7**. The C*H*$_2$N protons of the ligand resonate as an AX spin systems with δ_A ranging from 4.05 (**7**) to 4.11 (**5**) ppm and δ_X ranging from 4.38 (**5**) to 4.41 (**7**) ppm. The aromatic C*H* protons of the ligand resonate as two signals in the range of $\delta = 7.05$ to 7.37 ppm. To further vary the complexes, the electrophilic character of the Ge atom was altered. The reaction of **2** with two equivalents of $K[BEt_3H]$ yielded $\{[L(H)Ge]ZnCl(\mu\text{-}Cl)\}_2$ (**8**). Complex **8** has been characterized by NMR and IR spectroscopy. The ^{1}H NMR spectra of **8** ([D$_8$]THF) showed a new signal at $\delta = 6.40$ ppm due to the presence of Ge*H*. This signal is shifted upfield compared with its closest analogue, the monomeric complex Cu(*i*Pr-nacnac)-{GeH(*i*Pr-nacnac)}.[20b] The C*H*$_2$N protons of the ligand resonate as an AB spin system at $\delta = 4.28$ ppm, similarly to the starting complex **2**. The aromatic C*H* protons of the ligand resonate as two signals at $\delta = 7.20$ and 7.38 ppm. The IR spectra of **8** was measured in the solid state and the Ge*H* stretching band was

observed at 1964 cm^{-1}. This frequency is slightly lower than the one reported for N→Ge coordinated Ge^{II} hydride[26] and is very close to a carbene-capped digermene complex.[27] The molecular structures of **2** (M = Zn) and **3** (M = Cu) are found to be dimeric in the molecular structures with four-membered M_2Cl_2 rings.

In **2**, the central Zn atom is four-coordinate by three chloride ions Cl(2), Cl(2a), Cl(3), and the Ge(1) atom. The coordination polyhedron can be best described as a deformed tetrahedron with the bond angles Ge(1)-Zn(1)-Cl(3) (120.14(3)°) and Cl(2)-Zn(1)-Cl(2a) (95.14(1)°) with the biggest deviations from ideal shape. The Zn(1)–Cl(2) bond length (2.3454(9) Å) involved in the four-membered Zn_2Cl_2 ring is prolonged in comparison with the terminal Zn(1)–Cl(3) bond (2.2069(8) Å) (compare with Σ_{cov}Zn, Cl = 2.17 Å).[28] The Ge(1)–Zn(1) bond length (2.4615(5) Å) is comparable with the value (2.425(3) Å) found in the related complex depicted in Figure 1**IX**[22] and it is longer than the Ge–Zn covalent bond (Σ_{cov}Ge,Zn = 2.39 Å).[28–29] In complex **3** the central Cu atom is three-coordinate by two chloride ions Cl(2) and Cl(2a), and the Ge(1) atom. The coordination polyhedron can be best described as a deformed triangle with bond angles Ge(1)-Cu(1)-Cl(2) (136.08(2)°) and Cl(2)-Cu(1)-Cl(2a) (103.89(3)°) as representative of the biggest deviations from ideal shape. The Cu(1)-Cl(2) (2.2710(8) Å) and Cu(1)–Cl(2a) (2.3371(8) Å) bond lengths involved in Cu_2Cl_2 are slightly longer than a Cu–Cl covalent bond (Σ_{cov}Cu,Cl = 2.11 Å).[28] The Ge(1)–Cu(1) bond length (2.2700(5) Å) is comparable with the values found in the analogous Ge→Cu complexes (2.2765(8)–2.3788(16) Å)[20] and represent a strong Ge→Cu coordination; the bond length is even shorter than the Ge–Cu covalent bond (Σ_{cov}Ge,Cu = 2.33 Å).[28] The four-coordinate germanium atoms in **2** and **3** form distorted tetrahedral geometries. In both cases, the germanium atoms Ge(1) are connected to the carbon C(1) and nitrogen N(1) atom of the ligand, to the transition metal M (M = Zn(**2**), Cu(**3**)) and to one chlorine atom. The Ge(1)–N(1) bond lengths (2.047(2) Å (**2**), 2.085(2) Å (**3**)) indicate the presence of N→Ge interactions.

The molecular structure of **7** provides evidence for its monomeric nature.

The central Cu(1) atom is three-coordinate by one iodide ion I(1) and two germanium atoms. The coordination polyhedron is a deformed triangle with bond angles Ge(1)-Cu(1)-Ge(1a) (127.18(5)°) and I(1)-Cu(1)-Ge(1) (116.41(3)°) close to the ideal values. The Cu(1)–I(1) bond length (2.5051(18) Å) is close to that of a covalent bond (Σ_{cov}Cu, I = 2.47 Å).[28] The Ge(1)–Cu(1) bond length (2.3429(18) Å) is comparable with the values found in the analogous Ge→Cu complexes (2.2765(8)–2.3788(16) Å).[20] The value represents a strong Ge→Cu coordination (compare with Σ_{cov}Ge,Cu = 2.33 Å) but is longer than the corresponding appropriate value found for the dimeric complex **3** (2.2700(5) Å). The germanium atom Ge(1) is four-coordinate by carbon C(1) and nitrogen N(1) of the ligand as well as by one chlorine and Cu(1) atom. The Ge(1)–N(1) bond length (2.101(4) Å) indicates the presence of N→Ge interactions, similar to **2** and **3**.

The molecular structures of complex **1**–**8** were geometrically optimized with DFT (M06-2X/def2-TZVP). The bond lengths and angles for complexes **2**, **3**, and **7** displayed in Table 1 are in line with the values found in the crystal structures and show the reliability of the calculated results of the eight complexes. In addition to the optimized geometry, the NBO charges, Wiberg indices, and charge-transfer energies (CTE) were calculated (see the Supporting Information Tables S2 and S3).

The data allow the assessment of the bonding situation around the metal centers of the complexes. Herein, we see that the Ge–C and Ge–Cl bonds have a covalent character with Wiberg indices between 0.69–0.77 and very low or no charge-transfer energies. In contrast, the Ge–N and Ge–M interactions have a coordinative character. For the N→Ge coordination, the Wiberg indices lie between 0.28–0.37 and charge-transfer energies of up to 106 kcal mol^{-1} for **8** are reached. The coordination of Ge to Zn or Cu is characterized with Wiberg indices between 0.45–0.57 and charge-transfer energies up to 87 kcal mol^{-1}, again with **8** having the highest value. Since **8** distinguishes itself from the other complexes by being the only complex having a hydrogen atom bound to the Ge instead of a chloride, it can be concluded that this difference has a high impact on the electronical relations in the complex. Figure 4 gives the details of the bond situation of the Ge in

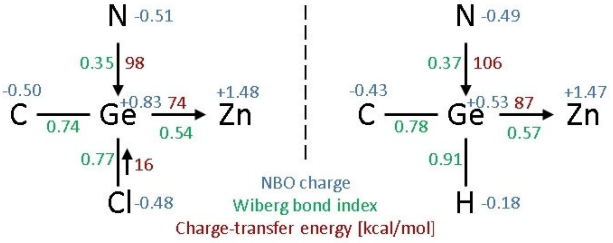

Figure 4. NBO charges, Wiberg bond indices and charge-transfer energies for the Ge coordination site in **2** (left) and **8** (right).

complex **2** and **8**, which only differ in Cl/H ligand. It fulfils the expectation, that the NBO charge of Ge in **8** is less positive than in **2** since the hydrogen atom has a weaker electronegativity and has hence a less electron-withdrawing character compared to Cl. With a Wiberg index of 0.91 and a NBO charge of −0.18, the hydrogen atom has a slightly hydridic character being covalently bound. This results in a stronger coordination of Ge to Zn in **8** as reflected by the higher charge-transfer energy. However, it is bizarre, that the C is left with a less negative charge, even though more electrons are available at the Ge atom. Furthermore, N coordinates with a higher charge-transfer energy, which should reflect a higher Lewis acidity of Ge and would be expected to correlate with the NBO charge of Ge. The exchange of the chloride ligand against the hydrogen atom comes along with the transformation of a covalent bond with strong ionic character (reflected by the Wiberg index and the charge-transfer energy) to a purely covalent bond. The big difference in the NBO charge of Ge probably is an artefact of the change of the kind of interaction and can, therefore, not be directly compared. Taking additionally the missing forth neighboring atom in **1** into account, the

Lewis acidity, which is known to be an important factor for the polymerization activity, is hence better comparable for all complexes by the strength of the N→Ge coordination, which is listed for **1**–**8** in Table S3 of the Supporting Information. The charge transfer-energies indicate the lowest Lewis acidity for **1**, the highest for **8** and the ones for complexes **2**–**7** in between.

For all complexes, a purely coordinative interaction is found between Ge and Zn or Cu. The difference of the chloride or the hydrogen atom bound to Ge is not reflected in the NBO charge of the Zn (+1.47 for **8**, +1.48 for **2**), even though Ge donates with different strengths. The charge of the Zn furthermore remains the same, if only one Zn is present (+1.46 for **5**). The NBO charges of Cu also stay in the same range. With iodine the Cu is slightly less positive (+0.65 and +0.64 for **4** and **7** versus +0.72 and +0.68 for **3** and **6**). According to charge-transfer energies (see Table S3, Supporting Information), the Ge→Zn donation in **2** is stronger in comparison with the dimeric Cu complexes **3** and **4**. This comparison must be regarded with some caution since **2** has terminal chorido donors and four iodido donors as bridging atoms, respectively. Overall, the Ge→M interactions are stronger in dimeric compounds in comparison with the related monomers.

The structures of complexes **1**–**8** allow a systematic investigation of the polymerization properties. By variation of the number of metal centers, the kind of metal as well as the halide ligands, these unique, advanced complexes will allow insights into the polymerization behavior of multimetal complexes.

Polymerizations

To investigate the relevance of the complexes for industrial application, the polymerization experiments were conducted solvent free in bulk at 150 °C. The monomer, L-lactide, was once recrystallized to avoid data fluctuations due to variation of impurities in technical grade lactide. The reactions were run in a stirred reactor at 260 rpm and monitored with in situ Raman spectroscopy. In accordance with other Zn catalysts,[10b] at first a *M*/*I* ratio of 500:1 was applied. After 1 min reaction time, a saturation due to high conversion was observable and after 4 min full conversion and molar masses above 50,000 g mol^{-1} were reached for complex **8** without addition of a co-initiator. These results were surprising, since organometallic compounds are often too sensitive to polymerize in bulk. Furthermore, the complexes showed robustness towards water, which is contained as an impurity in the recrystallized lactide. Similar results were obtained for the other complexes except for **1** which showed slower polymerization properties. To be able to quantify the polymerization activity and to differentiate their polymerization ability, the *M*/*I* ratio was increased until at 5000:1 the progress of the polymerization could be followed properly. In Figure 5 the semilogarithmic plot of the conversion against time for complexes **1**–**8** is shown.

The non-coordinating germylene moiety **1** shows a lower activity in the polymerization of lactide compared to **2**–**8**. The polymerization rate at a *M*/*I* ratio of 1000:1 is close to those of the other complexes at 5000:1. However, it has to be taken into account that the other complexes consist of multiple metal centers while **1** only has one Ge atom as an active site. In comparison with other Ge-complexes known from the literature, **1** shows an amazingly high polymerization activity.[14–16] So far Ge complexes have only been tested in bulk polymerization at a minimal *M*/*I* ratio of 600:1 and needed 24 h to reach a conversion of 70%. With a *M*/*I* ratio of 1000:1, **1** has already reached a conversion of 25% after one hour. The complex, therefore, provides a huge step in the category of Ge-only catalysts for the ring-opening polymerization of lactide.

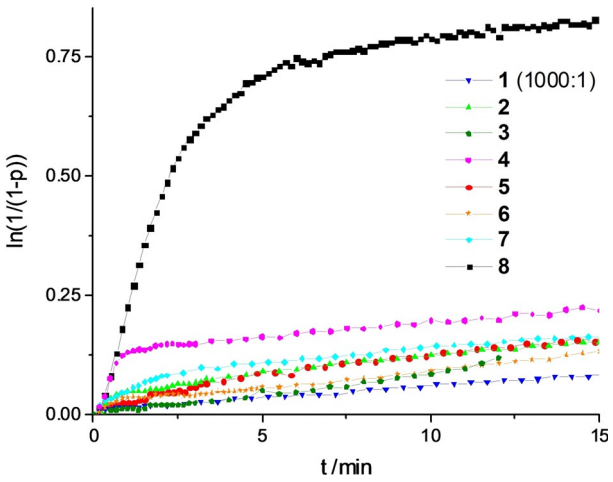

Figure 5. Semilogarithmic plot of complexes **1**–**8** with recrystallized L-lactide at 150 °C, 260 rpm, 5000:1 (except for **1**).

The complexes **2**–**8** contain two different metals, either Ge and Zn (**2**, **5**, **8**) or Ge and Cu (**3**, **4**, **6**, **7**). Since the germylene moiety **1** itself is able to polymerize under the given conditions, the active site of the polymetal complexes has to be identified. By the systematic variation of the complexes, indications for the influence of certain changes on the active site can be found. Four aspects are investigated: The kind of non-Ge metal center (Zn or Cu, **2** vs. **3**, **5** vs. **6**), influence of a second non-Ge metal center (**2** vs. **5**, **3** vs. **6**, **4** vs. **7**), the influence of the halide ligand (iodine or chlorine, **3** vs. **4**, **6** vs. **7**), and the influence of ligand on the Ge, chlorine or hydride (**2** vs. **8**).

The k_{obs} values of complexes **2**–**8** are shown in Table 2. When comparing the copper complexes with the zinc complexes, the polymerization activity does not differ taking the measurement inaccuracy into account. Usually it is found, that complexes with Cu are less active than the analogous zinc complexes.[30] This would be an indication that the non-Ge metal centers rather have a supporting role for Ge as active

Table 2. Observed reaction rate constants for complexes **2**–**8**.[a]

	2	**3**	**4**	
k_{obs} 10^{-4}/s^{-1}	1.47	1.40	0.93	
	5	**6**	**7**	**8**
k_{obs} 10^{-4}/s^{-1}	1.33	1.25	0.83	41.3

[a] Recrystallized L-lactide, 150 °C, 260 rpm, 5000:1.

polymerization sites. This is further supported by the negligible influence of a second non-Ge metal center: the reaction rate constant for **2**, **3**, and **4** is only approximately 10% higher compared to **5**, **6**, and **7**, respectively. It would be expected to be significantly higher, if Cu and Zn would be the active polymerization site. A cooperative effect as reported by Thevenon et al. is not observed.[23f] Theoretically, the bimetallic complexes could divide into two active sites with one ligand each having a fourfold coordination of the zinc or copper ion, a common coordination number for these metals. However, the little increase of the polymerization activity and no decrease of molar masses induced by a greater number of active sites (see Table S5 in Supporting Information) make the division of the complexes very unlikely. The addition of a second metal center is in total not very effective, which would be expected if Zn or Cu would be active in the polymerization. Unlike the first two factors, the influence of the different halide bound to the Cu atoms is well visible. If iodine acts as ligand to copper, the polymerization activity of the complex is decreased by 30%. This could have electronic reasons or stereochemical ones, for example, that the size of iodine hinders the approach of lactide to the active site. The greatest influence, however, is found in the exchange of the chloride ligand for a hydrogen at the Ge atoms. The observed reaction rate constant is raised by two magnitudes from **2** to **8**. The change of the electronic environment of the Ge leads to a massive increase of the polymerization activity. The polymerization property, therefore, correlates with the trend of the Lewis acidity found by DFT calculation. Compound **1** shows the lowest Lewis acidity and polymerizes the slowest, the activity of the complexes **2**–**7** are in a middle range and **8** excels all other complexes. The correlation of the theoretically determined parameters around the Ge atom with the polymerization activity of the complexes while the electronical situations of Zn and Cu remain constant, makes it very likely that Ge is the active site of the polymerization, which is further supported by MALDI-ToF-MS results (vide supra).

To compare the polymerization activity properly with other relevant catalysts, the k_p of complex **8** was determined (see Figure 6). The data points of the plot are fitted well by a straight line, which supports that the polymerization follows pseudo-first-order kinetics. A comparable value of k_p for the industrially used $Sn(Oct)_2$ was published recently with $k_p[Sn(Oct)_2] = (0.084 \pm 0.02)\ L\,mol^{-1}\,s^{-1}$.[10a] In comparison with $Sn(Oct)_2$, **8** shows a polymerization activity of two magnitudes higher, which is a great result compared to other Ge catalysts known for lactide polymerization, especially due to the industrial relevant conditions applied in this case.[17–18] Additionally, in comparison with other Zn catalysts, the reaction rate is impressive, since such high activities are mostly only found when polymerizing in solution at lower temperatures.[23f] The molar masses of the polymers produced by **8** (see the Supporting Information, Table S4, entries 8–15) are with more than 100 000 g mol^{-1} well suited for industrial processing. Due to the high activity of the complexes, it was not possible to stop the polymerization at different reaction times to monitor the growth of the polymer chains with the conversion. When comparing the resulting polymers of *M*/*I* ratio of 500:1 with 1000:1, the molar masses are approximately doubled as expected and lie in both cases close to the theoretical molar masses. With higher *M*/*I* ratios the molar masses are always found to be smaller than the theoretical values and do not exceed 120 000 g mol^{-1}. The growth of the polymer chain is hindered beyond this point due to the high viscosity and diffusion limitation in the bulk. Additionally, it is possible, that as a side effect of the high polymerization activity, complex **8** is also active in depolymerization. Especially for long reaction times (Table S4, entries 14 and 15, Supporting Information) shorter chains are obtained due to depolymerization besides higher *M*/*I* ratios. Side reactions like inter- and intramolecular transesterifications, which broaden the molar mass distribution, are more likely to occur when the chains are closer to each other; therefore, higher polydispersities (*PD*s) are found at higher conversion. Complexes **1**–**7** produce high molar mass polymers in a similar manner to **8**. Complex **1** needs to be stressed, because with an in comparison small *M*/*I* ratio of 1000:1 it produces polymers with molar masses in the same range as the other catalysts with an *M*/*I* ratio of 5000:1.

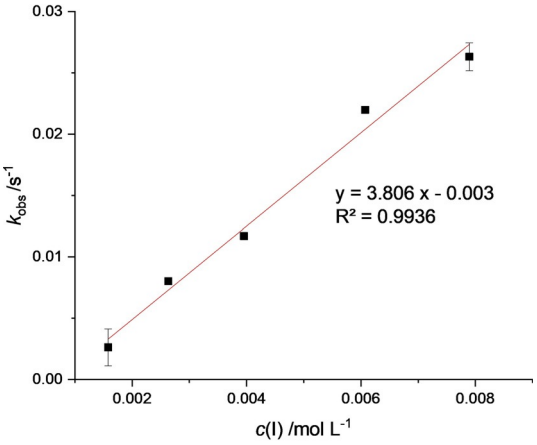

Figure 6. Determination of k_p of complex **8**. With *M*/*I* ratios between 1000:1 and 5000:1 at 150 °C, 260 rpm. $k_p(\mathbf{8}) = (3.806 \pm 0.315)\ L\,mol^{-1}\,s^{-1}$.

To investigate on the initiation mechanism, end group analyses were conducted using MALDI-ToF-MS. Samples with very short polymer chains were prepared with and without coinitiators of **2**, **5**, and **8**. The results are summarized in Table S5, Supporting Information. Interestingly, a wide range of end groups can be found: For all catalysts residual water in the recrystallized lactide acts as initiator and is found as a hydroxyl end group. If an extra coinitiator like benzyl alcohol is added to the polymerization mixture, it also initiates chain growth. The in total larger number of initiated polymer chains leads to a reduced average molar mass compared to the polymerization without coinitiator. The catalyst itself is found in different variations at the chain ends. Especially the L-Ge end group is interesting, since it shows, that the polymer chain grows on the Ge atom, independently of the Zn atom. Since it is unlikely that the Ge acts as nucleophile in the ring-opening step, it supports the argument of Ge being the active site of the polymerization at which the chain starts growing. The end groups of the different catalysts do not differ significantly, which un-

derlines the redundancy of the second Zn atom in **2**. The presence of water in the end group analysis refers to the need of a nucleophile for the polymerization, which is the case for the coordination–insertion mechanism. This mechanism is described by pseudo-first-order kinetics since the number of active sites is constant during the polymerization. The equations fit the data for k_{obs} and k_p determination very well and when plotting the logarithmic k_{obs} values of the k_p determination for **8** against the logarithmic initiator concentration, the slope, which corresponds to the reaction order, is found to be close to 1 (see the Supporting Information Figure S3). Therefore, it can be concluded, that the complexes polymerize with first-order kinetics after the coordination–insertion mechanism.

For all complexes it was observed, that with time a deactivation takes place even though full conversion is not yet reached (see Figure 5 for **8** and Figure S2 in the Supporting Information for **1**–**7**). All complexes were, therefore, investigated with thermogravimetric analysis (see the Supporting Information Figure S4) to find, that the complexes are not stable for a long time at 150 °C. The deactivation observed in the polymerization is, therefore, an effect of the high temperature used for bulk polymerization of lactide. However, when taking a closer look at the polymerization results, it becomes clear, that the relevant data are collected during the first minutes, in which the complexes are still active as catalysts. Since the presented data are very well-fitted by the equations of a first-order kinetics, the complexes must be stable throughout the time of investigation and the validity of the assumptions made concerning the polymerization properties is maintained.

Conclusions

On the route towards a tin-free production of polylactide, eight germanium complexes were synthesized, characterized, and tested in the bulk polymerization of lactide. The structural variation of the complexes, concerning the non-Ge metals, the counter ions, and the number of metal atoms, allowed a systematic investigation of the structure–property relationships. The conducted kinetics in combination with end-group analysis lead to the conclusion that despite the presence of Zn or Cu in the complexes, Ge is the active site for polymerization following the coordination–insertion mechanism. With one complex showing a rate constant two magnitudes higher than $Sn(Oct)_2$ in the bulk polymerization under industrial relevant conditions, the potential of Ge catalyst as a substitute for the tin component is proven.

Experimental Section

General methods

Starting compound **1** was prepared according to the literature.[24] All reactions were carried out under argon, using standard Schlenk techniques. Complex $(CuI)_4{\cdot}(SMe_2)_3$, $ZnCl_2$, CuCl, and a 1 M THF solution of $K[BEt_3H]$ were purchased from Sigma Aldrich. Solvents were dried by standard methods and distilled prior to use. The ^1H and $^{13}C\{^1H\}$ NMR spectra were recorded at ambient temperature with a Bruker Avance 500 spectrometer. The chemical shifts δ are given in ppm and referenced to external $SiMe_4$ (^1H, ^{13}C). IR spectra were recorded on a Nicolet 6700 FTIR spectrometer by using single-bounce diamond ATR crystal (resolution 2 cm^{-1}); the spectrometer and sample compartment was purged with dry air during all experiments. The TG experiments were performed with a thermogravimetric analyzer (Pyris 1 TGA HT, PerkinElmer) by heating samples from 310 to 473 K at a ramp rate of 10 °C min^{-1} under a nitrogen flow at 20 mL min^{-1}.

Synthesis of $\{[L(Cl)Ge]ZnCl(\mu\text{-}Cl)\}_2$ (2)

Compound **1** (1.78 g, 4.65 mmol) and $ZnCl_2$ (0.63 g, 4.65 mmol) were dissolved in 20 mL of THF and stirred at room temperature for 1 h. The organic solvents were evaporated and 15 mL of hexane was added. The resulting suspension was filtered and the white solid dried in vacuum. Yield: 2.39 g (99%), m.p. 222–224 °C (decomp); ^1H NMR (500.13 MHz, $CDCl_3$, 300K): $\delta = 1.23$ (br, 3H CH_2CH_3,), 1.31 (s, 9H, $C(CH_3)_3$), 1.44 (br, 3H, CH_2CH_3), 1.49 (s, 9H, $C(CH_3)_3$), 3.17 (m, 1H, CH_2CH_3), 3.39 (m, 1H, CH_2CH_3), 3.54 (m, 1H, CH_2CH_3), 3.61 (br, 1H, CH_2CH_3), 4.20 (br, 1H, CH_2N), 4.33 (m, 1H, CH_2N), 7.09 (s, 1H, Ar*H*), 7.43 ppm (s, 1H, Ar*H*), $^{13}C\{^1H\}$ NMR (125.77 MHz, $CDCl_3$, 300K): $\delta = 9.6$, 11.1, 31.4, 33.6, 35.1, 37.4, 47.1, 50.1, 60.7 (CH_2N), 119.1, 123.5, 139.2, 141.5, 154.0, 156.8 ppm.

Synthesis of $\{[L(Cl)Ge]Cu(\mu\text{-}Cl)\}_2$ (3)·C_6H_6

Compound **1** (2.04 g, 5.33 mmol) and CuCl (0.53 g, 5.33 mmol) were dissolved in 15 mL of benzene and stirred at room temperature for 48 h. The suspension was filtrated and white solid dried in vacuum. Yield: 2.55 g (92%); m.p. 186–189 °C (decomp); ^1H NMR (500.13 MHz, $CDCl_3$, 300K): $\delta = 1.18$ (m, 3H, CH_2CH_3), 1.30 (s, 9H, $C(CH_3)_3$), 1.37 (m, 3H, CH_2CH_3), 1.55 (s, 9H, $C(CH_3)_3$)„ 3.05 (m, 2H, CH_2CH_3), 3.53 (m, 2H, CH_2CH_3), 4.19 (m, 2H, CH_2N), 7.03 (s, 1H, Ar*H*), 7.37 (s, 1H, Ar*H*), 7.37 ppm (s, 6H, benzene); $^{13}C\{^1H\}$ NMR (125.77 MHz, $CDCl_3$, 300K): $\delta = 8.5$, 11.6, 31.4, 33.7, 35.0, 37.6, 44.7, 48.5, 60.6 (CH_2N), 118.8, 122.3, 142.0, 143.2, 152.7, 156.6, 128.5 ppm (benzene).

Synthesis of $\{[L(Cl)Ge]Cu(\mu\text{-}I)\}_2$ (4)·C_6H_6

Compound **1** (1.16 g, 3.03 mmol) and $(CuI)_4{\cdot}(SMe_2)_3$ (0.72 g, 0.76 mmol) were dissolved in 15 mL of benzene and stirred at room temperature for 48hrs. The suspension was filtrated and white solid dried in vacuum. Yield: 3.45 g (93%); m.p. 174–177 °C (decomp); ^1H NMR (500.13 MHz, $CDCl_3$, 300K): $\delta = 1.10$ (t, 3H, ^2J(1H, 1H) = 7.0 Hz, CH_2CH_3), 1.26 (s, 9H, $C(CH_3)_3$), 1.42 (t, 3H, ^2J(1H, 1H) = 7.0 Hz, CH_2CH_3), 1.52 (s, 9H, $C(CH_3)_3$), 2.95 (m, 1H, CH_2CH_3), 3.14 (m, 1H, CH_2CH_3), 3.60 (m, 2H, CH_2CH_3), 3.99 (AX spin system, 1H, CH_2N, ^2J(1H, 1H) = 14.1 Hz), 4.35 (AX spin system, 1H, CH_2N, ^2J(1H, 1H) = 14.1 Hz), 7.00 (s, 1H, Ar*H*), 7.30 (s, benzene), 7.31 ppm (s, 1H, Ar*H*); $^{13}C\{^1H\}$ NMR (125.77 MHz, $CDCl_3$, 300K): $\delta = 8.2$, 12.4, 31.5, 34.0, 35.0, 37.5, 45.4, 48.3, 60.8 (CH_2N), 118.9, 122.4, 142.2, 144.1, 152.7, 156.5, 128.5 ppm (benzene).

Synthesis of $[L(Cl)Ge]_2ZnCl_2$ (5)

Compound **1** (1.70 g, 4.44 mmol) and $ZnCl_2$ (0.30 g, 2.22 mmol) were dissolved in 20 mL of THF and stirred at room temperature for 1 h. The organic solvents were evaporated and 15 mL of hexane was added. The resulting suspension was filtered and the white solid dried in vacuum. Alternatively, compound **1** (1.22 g, 3.19 mmol) and complex **2** (1.65 g, 1.16 mmol) were dissolved in THF and stirred at room temperature for 1 h. The organic solvents were evaporated and 15 mL of hexane was added. The resulting

suspension was filtrated and the resulting white solid dried under vacuum. Yield: 1.98 g (99%); m.p. 208–210 °C (decomp); ^{1}H NMR (500.13 MHz, $CDCl_3$, 300K): $\delta = 1.20$ (br, 3H, CH_2CH_3), 1.29 (s, 9H, $C(CH_3)_3$), 1.32 (br, 3H, CH_2CH_3), 1.49 (s, 9H, $C(CH_3)_3$), 3.01 (m, 1H, CH_2CH_3), 3.29 (m, 2H, CH_2CH_3), 3.58 (m, 1H, CH_2CH_3), 4.11 (br, 1H, CH_2N), 4.38 (br, 1H, CH_2N), 7.07 (s, 1H, Ar*H*), 7.36 ppm (s, 1H, Ar*H*), ^{13}C{^{1}H} NMR (125.77 MHz, $CDCl_3$, 300K): $\delta = 9.1$, 10.8, 31.4, 33.6, 35.0, 37.4, 45.2, 48.6, 61.3 (CH_2N), 118.8, 122.5, 142.5, 144.8, 152.7, 156.5 ppm.

Synthesis of [L(Cl)Ge]$_2$CuCl (6)·C$_6$H$_6$

Compound **1** (2.36 g, 6.17 mmol) and CuCl (0.305 g, 3.08 mmol) were dissolved in 15 mL of benzene and stirred at room temperature for 48 h. The suspension was filtrated and white solid dried in vacuum. Alternatively, compound **1** (0.82 g, 2.14 mmol) and complex **3** (1.12 g, 1.07 mmol) were dissolved in CH_2Cl_2 and 0.1 mL benzene and stirred at room temperature for 1 h. The organic solvents were evaporated. Yield: 2.70 g (93%); m.p. 158–160 °C (decomp); ^{1}H NMR (500.13 MHz, $CDCl_3$, 300 K): $\delta = 1.14$ (t, 3H, ^2J(1H, 1H) = 6.9 Hz, CH_2CH_3), 1.31 (s, 9H, $C(CH_3)_3$), 1.50 (t, 3H, ^{2}J(1H, 1H) = 6.9 Hz, CH_2CH_3), 1.59 (s, 9H, $C(CH_3)_3$), 2.95 (m, 1H, CH_2CH_3), 3.14 (m, 1H, CH_2CH_3), 3.63 (m, 1H, CH_2CH_3), 3.77 (m, 1H, CH_2CH_3), 4.05 (AX spin system, 1H, CH_2N, ^2J(1H, 1H) = 14.0 Hz), 4.39 (AX spin system, 1H, CH_2N, ^2J(1H, 1H) = 14.0 Hz), 7.05 (s, 1H, Ar*H*), 7.36 (s, 1H, benzene), 7.37 ppm (s, 1H, Ar*H*); ^{13}C{^{1}H} NMR (125.77 MHz, $CDCl_3$, 300K): $\delta = 7.8$, 12.3, 31.4, 33.9, 35.0, 37.5, 44.2, 48.2, 60.6 (CH_2N), 118.9, 122.2, 142.1, 144.0, 152.6, 156.4, 128.4 ppm (benzene).

Synthesis of [L(Cl)Ge]$_2$CuI (7)·C$_6$H$_6$

Compound **1** (1.28 g, 3.35 mmol) and $(CuI)_4$·$(SMe_2)_3$ (0.40 g, 0.42 mmol) were dissolved in 15 mL of benzene and stirred at room temperature for 48 h. The suspension was filtrated and white solid dried in vacuum. Alternatively, compound **1** (0.63 g, 1.65 mmol) and complex **4** (1.01 g, 0.82 mmol) were dissolved in CH_2Cl_2 and 0.1 mL benzene and stirred at room temperature for 1 h. The organic solvents were evaporated. Yield: 1.64 g (95%); m.p. 175–178 °C (decomp); ^{1}H NMR (500.13 MHz, $CDCl_3$, 300K): $\delta =$ 1.14 (t, 3H, ^2J(1H, 1H) = 7.2 Hz, CH_2CH_3), 1.31 (s, 9H, $C(CH_3)_3$), 1.49 (t, 3H, ^2J(1H, 1H) = 7.2 Hz, CH_2CH_3), 1.57 (s, 9H, $C(CH_3)_3$), 2.99 (m, 1H, CH_2CH_3), 3.14 (m, 1H, CH_2CH_3), 3.64 (m, 1H, CH_2CH_3), 3.77 (m, 1H, CH_2CH_3), 4.05 (AX spin system, 1H, CH_2N, ^2J(1H, 1H) = 14.2Hz), 4.41 (AX spin system, 1H, CH_2N, ^2J(1H, 1H) = 14.2Hz), 7.05 (s, 1H, Ar*H*), 7.36 (s, 1H, Ar*H*), 7.36 ppm (s,2H, benzene); ^{13}C{^{1}H} NMR (125.77 MHz, $CDCl_3$, 300 K): $\delta = 8.1$, 12.4, 31.5, 34.0, 35.0, 37.5, 45.3, 48.2, 60.8 (CH_2N), 118.9, 122.4, 142.2, 144.3, 152.7, 156.5, 128.5 ppm (benzene).

Synthesis of {[L(H)Ge]ZnCl(μ-Cl)}$_2$ (8)

Compound **2** (1.63 g, 1.57 mmol) was dissolved in 20 mL of THF and cooled to −30 °C. Then 1 M THF solution of K[Bet$_3$H] (3.14 mL, 3.14 mmol) was added and the reaction mixture was stirred for 1 h at −30 °C. The organic solvents were evaporated, 10 mL of hexane was added and resulting suspension was filtered. Solid material was dissolved in 15 mL of benzene, filtered, and the filtrate was evaporated to dryness. The resulting white crystalline substance was characterized. Yield: 1.11 g (73%); m.p. 147–150 °C (decomp); ^{1}H NMR (500.13 MHz, [D$_8$]THF, 300K): $\delta = 1.16$ (br, 3H, CH_2CH_3), 1.26 (br, 3H, CH_2CH_3), 1.30 (s, 9H, $C(CH_3)_3$), 1.33 (s, 9H, $C(CH_3)_3$), 3.10 (m, 1H, CH_2CH_3), 3.24 (m, 1H, CH_2CH_3), 3.32 (m, 1H, CH_2CH_3), 3.71 (m, 1H, CH_2CH_3), 4.24 (AB spin system, 1H, CH_2N, ^2J(1H, 1H) = 13.8Hz), 4.33 (AB spin system, 1H, CH_2N, ^2J(1H, 1H) = 13.8Hz), 6.40 (s, 1H, Ge*H*), 7.20 (s, 1H, Ar*H*), 7.38 ppm (s, 1H, Ar*H*); ^{13}C{^{1}H} NMR (125.77 MHz, [D$_8$]THF, 300K): $\delta = 8.9$, 11.9, 31.5, 32.0, 35.1, 37.2, 50.4, 62.3 (CH_2N), 119.7, 122.9, 137.2, 141.9, 151.8, 155.9 ppm, IR $\nu =$ 1964 (GeH) cm^{-1}.

Polymerization procedure in bulk

In a nitrogen filled glove box, recrystallized L-lactide (8.0 g, 55.5 mmol) and the catalyst were weighted in and mixed in a mortar. The reaction mixture was filled in a glass vial and removed from the glovebox. The reactor was heated at 150 °C under vacuum and flashed three times with argon. The reaction was conducted under argon atmosphere and sample collection started after the reaction mixture insertion as soon as the reactor was closed. The spectra were measured with a RXN1 spectrometer of Kaiser Optical Systems. The laser was used at a wavelength 785 nm and 450 mW through a probe head with sapphire lenses ($d =$ 0.1 mm). The reaction time was adjusted to the [*M*]/[*I*]-ratio. The reaction mixture was removed from the reactor and a ^{1}H NMR spectrum was collected to determine the conversion. The reaction mixture was dissolved in an appropriate amount of DCM, the polymer was precipitated in ethanol at room temperature, dried under vacuum, and characterized via GPC. Kinetic data were obtained by integration of the Raman spectrum with *Peaxact 4,* boundaries were 627–713 cm^{-1} for lactide.

Computational details

The geometry optimizations were started from the geometry of the solid-state structures by using the M06-2x functional[31a] and with the Ahlrichs type basis set def2-TZVP[31b–d] basis set as implemented in Gaussian 16.[32] NBO calculations were accomplished using the program suite NBO 6.0 delivering the charge-transfer energies by second order perturbation theory.[33]

Crystallography

The X-ray data for single crystals of **2**, **3**·C$_6$H$_6$ and **7**·C$_6$H$_6$ were obtained at 150 K using Oxford Cryostream low-temperature device on a Nonius KappaCCD diffractometer with $Mo_{K\alpha}$ radiation ($\lambda =$ 0.71073 Å), a graphite monochromator, and the φ and χ scan mode. Crystals of **2**, **3**·C$_6$H$_6$, and **7**·C$_6$H$_6$ were obtained from saturated benzene solutions of the parent complexes at room temperature. Data reductions were performed with DENZO-SMN.[34] The absorption was corrected by integration methods.[35] Structures were solved by direct methods (Sir92)[35] and refined by full matrix least-square based on F^2 (SHELXL97).[36] Hydrogen atoms were mostly localized on a difference Fourier map, however to ensure uniformity of treatment of crystal, all hydrogen were recalculated into idealized positions (riding model) and assigned temperature factors $H_{iso}(H) = 1.2\ U_{eq}$ (pivot atom) or of $1.5\ U_{eq}$ (methyl). H atoms in methyl, methylene, methine moieties and hydrogen atoms in aromatic rings were placed with C–H distances of 0.96, 0.97, 0.98, and 0.93.

CCDC 1948324, 1948325, and 1948326 (**2**, **3**·C$_6$H$_6$, **7**·C$_6$H$_6$, respectively) contain the supplementary crystallographic data for this paper. These data are provided free of charge by The Cambridge Crystallographic Data Centre.

Acknowledgements

R.D.R. thanks the DBU (Deutsche Bundesstiftung Umwelt) for funding. The authors acknowledge funding by the Deutsche Forschungsgemeinschaft in the framework of the SFB985, TACR (project no. TH02010197) and thank Total Corbion for lactide donations. We furthermore thank the Paderborn Center for Parallel Computing, PC^2, for providing computing time on the High-Performance Computing (HPC) system OCuLUS as well as support.

Conflict of interest

The authors declare no conflict of interest.

Keywords: bioplastics · germanium · lactide · ring-opening polymerization · zinc

[1] a) C. Schmidt, T. Krauth, S. Wagner, *Environ. Sci. Technol.* **2017**, *51*, 12246 – 12253; b) L. C. Lebreton, J. Van der Zwet, J.-W. Damsteeg, B. Slat, A. Andrady, J. Reisser, *Nat. Commun.* **2017**, *8*, 15611; c) P. Bhattacharya, S. Lin, J. P. Turner, P. C. Ke, *J. Phys. Chem. C* **2010**, *114*, 16556 – 16561; d) A. L. Cardozo, E. G. Farias, J. L. Rodrigues-Filho, I. B. Moteiro, T. M. Scandolo, D. V. Dantas, *Mar. Pollut. Bull.* **2018**, *130*, 19 – 27; e) J. N. Hahladakis, C. A. Velis, R. Weber, E. Iacovidou, P. Purnell, *J. Hazard. Mater.* **2018**, *344*, 179 – 199.

[2] a) S. Brockhaus, M. Petersen, W. Kersten, *J. Cleaner Prod.* **2016**, *127*, 84 – 95; b) J. Payne, P. McKeown, M. D. Jones, *Polym. Degrad. Stab.* **2019**, *165*, 170 – 181; c) J. Wróblewska-Krepsztul, T. Rydzkowski, G. Borowski, M. Szczypiński, T. Klepka, V. K. Thakur, *Int. J. Polym. Anal. Charact.* **2018**, *23*, 383 – 395.

[3] a) G. Kale, R. Auras, S. P. Singh, R. Narayan, *Polym. Test.* **2007**, *26*, 1049 – 1061; b) R. E. Drumright, P. R. Gruber, D. E. Henton, *Adv. Mater.* **2000**, *12*, 1841 – 1846; c) M. Rabnawaz, I. Wyman, R. Auras, S. Cheng, *Green Chem.* **2017**, *19*, 4737 – 4753.

[4] a) W. J. Groot, T. Borén, *Int. J. Life Cycle Assess.* **2010**, *15*, 970 – 984; b) M. Itävaara, S. Karjomaa, J.-F. Selin, *Chemosphere* **2002**, *46*, 879 – 885; c) G. Kale, R. Auras, S. P. Singh, *J. Polym. Environ.* **2006**, *14*, 317 – 334; d) T. P. Haider, C. Völker, J. Kramm, K. Landfester, F. R. Wurm, *Angew. Chem. Int. Ed.* **2019**, *58*, 50 – 62; *Angew. Chem.* **2019**, *131*, 50 – 63.

[5] a) R. Auras, B. Harte, S. Selke, *Macromol. Biosci.* **2004**, *4*, 835 – 864; b) J. Gonzalez Ausejo, J. Rydz, M. Musioł, W. Sikorska, H. Janeczek, M. Sobota, J. Włodarczyk, U. Szeluga, A. Hercog, M. Kowalczuk, *Polym. Degrad. Stab.* **2018**, *156*, 100 – 110; c) S. Alippilakkotte, L. Sreejith, *J. Appl. Polym. Sci.* **2018**, *135*, 46056; d) Q. Jiang, X. Pei, L. Wu, T. T. Li, J. H. Lin, *Adv. Polym. Technol.* **2018**, *37*, 2971 – 2980.

[6] H. Endres, A. Siebert-Raths, H. Behnsen, C. Schulz, *Biopolymers: Facts and Statistics*, Hanover, **2016**.

[7] a) N. E. Kamber, W. Jeong, R. M. Waymouth, R. C. Pratt, B. G. Lohmeijer, J. L. Hedrick, *Chem. Rev.* **2007**, *107*, 5813 – 5840; b) H. R. Kricheldorf, I. Kreiser-Saunders, C. Boettcher, *Polymer* **1995**, *36*, 1253 – 1259.

[8] a) R. J. Lewis, N. Sax, *Sax's Dangerous Properties of Industrial Materials, Vol. 12*, New York, **1996**; b) M. D. Jones, X. Wu, J. Chaudhuri, M. G. Davidson, M. J. Ellis, *Mater. Sci. Eng. C* **2017**, *80*, 69 – 74.

[9] a) V. Poirier, T. Roisnel, J.-F. Carpentier, Y. Sarazin, *Dalton Trans.* **2009**, 9820 – 9827; b) A. B. Biernesser, B. Li, J. A. Byers, *J. Am. Chem. Soc.* **2013**, *135*, 16553 – 16560; c) O. J. Driscoll, C. K. Leung, M. F. Mahon, P. McKeown, M. D. Jones, *Eur. J. Inorg. Chem.* **2018**, 5129 – 5135; d) C. K. Williams, L. E. Breyfogle, S. K. Choi, W. Nam, V. G. Young, M. A. Hillmyer, W. B. Tolman, *J. Am. Chem. Soc.* **2003**, *125*, 11350 – 11359; e) J.-C. Buffet, A. Kapelski, J. Okuda, *Macromolecules* **2010**, *43*, 10201 – 10203; f) A. Stopper, J. Okuda, M. Kol, *Macromolecules* **2012**, *45*, 698 – 704; g) A. Pilone, K. Press, I. Goldberg, M. Kol, M. Mazzeo, M. Lamberti, *J. Am. Chem. Soc.* **2014**, *136*, 2940 – 2943; h) P. Steiniger, P. M. Schäfer, C. Wölper, J. Henkel, A. N. Ksiazkiewicz, A. Pich, S. Herres-Pawlis, S. Schulz, *Eur. J. Inorg. Chem.* **2018**, 4014 – 4021; i) T. Rosen, I. Goldberg, V. Venditto, M. Kol, *J. Am. Chem. Soc.* **2016**, *138*, 12041 – 12044; j) J. Y. C. Lim, N. Yuntawattana, P. D. Beer, C. K. Williams, *Angew. Chem. Int. Ed.* **2019**, *58*, 6007 – 6011; *Angew. Chem.* **2019**, *131*, 6068 – 6072; k) Z. Zhong, P. J. Dijkstra, J. Feijen, *Angew. Chem. Int. Ed.* **2002**, *41*, 4510 – 4513; *Angew. Chem.* **2002**, *114*, 4692 – 4695.

[10] a) R. D. Rittinghaus, P. M. Schäfer, P. Albrecht, C. Conrads, A. Hoffmann, A. N. Ksiazkiewicz, O. Bienemann, A. Pich, S. Herres-Pawlis, *ChemSusChem* **2019**, *12*, 2161 – 2165; b) P. Schäfer, M. Fuchs, A. Ohligschläger, R. Rittinghaus, P. McKeown, E. Akin, M. Schmidt, A. Hoffmann, M. Liauw, S. Herres-Pawlis, *ChemSusChem* **2017**, *10*, 3547 – 3556; c) P. M. Schäfer, P. McKeown, M. Fuchs, R. D. Rittinghaus, A. Hermann, J. Henkel, S. Seidel, C. Roitzheim, A. N. Ksiazkiewicz, A. Hoffmann, A. Pich, M. D. Jones, S. Herres-Pawlis, *Dalton Trans.* **2019**, *48*, 6071 – 6082; d) C. J. Chuck, M. G. Davidson, G. Gobius du Sart, P. K. Ivanova-Mitseva, G. I. Kociok-Köhn, L. B. Manton, *Inorg. Chem.* **2013**, *52*, 10804 – 10811.

[11] S. de Vos, P. Jansen, in *8th World Congress of Chemical Engineering* **2009**.

[12] a) U. Herber, K. Hegner, D. Wolters, R. Siris, K. Wrobel, A. Hoffmann, C. Lochenie, B. Weber, D. Kuckling, S. Herres-Pawlis, *Eur. J. Inorg. Chem.* **2017**, 1341 – 1354; b) X. Wang, K. Liao, D. Quan, Q. Wu, *Macromolecules* **2005**, *38*, 4611 – 4617; c) M. Stolt, A. Södergård, *Macromolecules* **1999**, *32*, 6412 – 6417; d) P. Marin, M. Tschan, F. Isnard, C. Robert, P. Haquette, X. Trivelli, L.-M. Chamoreau, V. Guérineau, I. del Rosal, C. M. Thomas, *Angew. Chem. Int. Ed.* **2019**, *58*, 12585 – 12589; *Angew. Chem.* **2019**, *131*, 12715 – 12719.

[13] a) S. J. Halperin, A. Barzilay, M. Carson, C. Roberts, J. Lynch, S. Komarneni, *J. Plant Nutr.* **1995**, *18*, 1417 – 1426; b) G. B. Gerber, A. Léonard, *Mutat. Res.* **1997**, *387*, 141 – 146.

[14] H. R. Kricheldorf, D. Langanke, *Polymer* **2002**, *43*, 1973 – 1977.

[15] A. Finne, A. C. Albertsson, *J. Polym. Sci. Part A* **2003**, *41*, 3074 – 3082.

[16] a) A. J. Chmura, C. J. Chuck, M. G. Davidson, M. D. Jones, M. D. Lunn, S. D. Bull, M. F. Mahon, *Angew. Chem. Int. Ed.* **2007**, *46*, 2280 – 2283; *Angew. Chem.* **2007**, *119*, 2330 – 2333.

[17] a) J. Guo, P. Haquette, J. Martin, K. Salim, C. M. Thomas, *Angew. Chem. Int. Ed.* **2013**, *52*, 13584 – 13587; *Angew. Chem.* **2013**, *125*, 13829 – 13832.

[18] L. Wang, S.-C. Roşca, V. Poirier, S. Sinbandhit, V. Dorcet, T. Roisnel, J.-F. Carpentier, Y. Sarazin, *Dalton Trans.* **2014**, *43*, 4268 – 4286.

[19] S. M. Weidner, H. R. Kricheldorf, *J. Polym. Sci. Part A* **2018**, *56*, 2730 – 2738.

[20] a) S. Bestgen, N. H. Rees, J. M. Goicoechea, *Organometallics* **2018**, *37*, 4147 – 4155; b) H. Arii, F. Nakadate, K. Mochida, *Organometallics* **2009**, *28*, 4909 – 4911; c) L. Ferro, P. B. Hitchcock, M. P. Coles, J. R. Fulton, *Inorg. Chem.* **2012**, *51*, 1544 – 1551; d) N. Zhao, J. Zhang, Y. Yang, H. Zhu, Y. Li, G. Fu, *Inorg. Chem.* **2012**, *51*, 8710 – 8718; e) J. K. West, G. L. Fondong, B. C. Noll, L. Stahl, *Dalton Trans.* **2013**, *42*, 3835 – 3842; f) D. Yadav, R. K. Siwatch, S. Sinhababu, S. Nagendran, *Inorg. Chem.* **2013**, *52*, 600 – 606; g) J. Hlina, H. Arp, M. Walewska, U. Flörke, K. Zangger, C. Marschner, J. Baumgartner, *Organometallics* **2014**, *33*, 7069 – 7077; h) W.-P. Leung, C.-W. So, K.-H. Chong, K.-W. Kan, H.-S. Chan, T. C. Mak, *Organometallics* **2006**, *25*, 2851 – 2858; i) J. T. York, V. G. Young, W. B. Tolman, *Inorg. Chem.* **2006**, *45*, 4191 – 4198; j) N. Zhao, J. Zhang, Y. Yang, G. Chen, H. Zhu, H. W. Roesky, *Organometallics* **2013**, *32*, 762 – 769; k) A. E. Ayers, H. R. Dias, *Inorg. Chem.* **2002**, *41*, 3259 – 3268; l) H. R. Dias, Z. Wang, *Inorg. Chem.* **2000**, *39*, 3890 – 3893.

[21] a) L. A. Álvarez-Rodríguez, J. A. Cabeza, P. García-Álvarez, D. Polo, *Organometallics* **2015**, *34*, 5479 – 5484; b) C. Seow, M. L. B. Ismail, H.-W. Xi, Y. Li, K. H. Lim, C.-W. So, *Organometallics* **2018**, *37*, 1368 – 1372.

[22] a) S. Sinhababu, D. Yadav, S. Karwasara, M. K. Sharma, G. Mukherjee, G. Rajaraman, S. Nagendran, *Angew. Chem. Int. Ed.* **2016**, *55*, 7742 – 7746; *Angew. Chem.* **2016**, *128*, 7873 – 7877.

[23] a) J. Börner, U. Flörke, K. Huber, A. Döring, D. Kuckling, S. Herres-Pawlis, *Chem. Eur. J.* **2009**, *15*, 2362 – 2376; b) J. Börner, I. dos Santos Vieira, M. D. Jones, A. Döring, D. Kuckling, U. Flörke, S. Herres-Pawlis, *Eur. J. Inorg. Chem.* **2011**, 4441 – 4456; c) M. D. Jones, M. G. Davidson, C. G. Keir, L. M. Hughes, M. F. Mahon, D. C. Apperley, *Eur. J. Inorg. Chem.* **2009**, 635 – 642; d) C. Di Iulio, M. D. Jones, M. F. Mahon, D. C. Apperley, *Inorg. Chem.* **2010**, *49*, 10232 – 10234; e) T. Rosen, Y. Popowski, I. Goldberg, M. Kol, *Chem. Eur. J.* **2016**, *22*, 11533 – 11536; f) A. Thevenon, C. Romain, M. S. Bennington, A. J. White, H. J. Davidson, S. Brooker, C. K. Williams, *Angew. Chem. Int. Ed.* **2016**, *55*, 8680 – 8685; *Angew. Chem.* **2016**, *128*, 8822 – 8827.

[24] a) J. Tremmel, L. Dostál, M. Erben, Z. Růžičková, J. Turek, F. De Proft, R. Jambor, *Eur. J. Inorg. Chem.* **2017**, 3100 – 3104; b) J. Tremmel, M. Erben, L. Dostal, Z. Ruzickova, J. Turek, R. Jambor, *Eur. J. Inorg. Chem.* **2019**, 1884 – 1894.
[25] M. Novák, M. Bouška, L. Dostál, A. Růžička, A. Hoffmann, S. Herres-Pawlis, R. Jambor, *Chem. Eur. J.* **2015**, *21*, 7820 – 7829.
[26] S. Khan, P. P. Samuel, R. Michel, J. M. Dieterich, R. A. Mata, J.-P. Demers, A. Lange, H. W. Roesky, D. Stalke, *Chem. Commun.* **2012**, *48*, 4890 – 4892.
[27] S. I. Al-Rafia, M. R. Momeni, M. J. Ferguson, R. McDonald, A. Brown, E. Rivard, *Organometallics* **2013**, *32*, 6658 – 6665.
[28] a) P. Pyykkö, M. Atsumi, *Chem. Eur. J.* **2009**, *15*, 186 – 197; b) P. Pyykkö, M. Atsumi, *Chem. Eur. J.* **2009**, *15*, 12770 – 12779.
[29] J. D. Erickson, R. D. Riparetti, J. C. Fettinger, P. P. Power, *Organometallics* **2016**, *35*, 2124 – 2128.
[30] a) S. Bhunora, J. Mugo, A. Bhaw-Luximon, S. Mapolie, J. Van Wyk, J. Darkwa, E. Nordlander, *Appl. Organomet. Chem.* **2011**, *25*, 133 – 145; b) D. Appavoo, B. Omondi, I. A. Guzei, J. L. van Wyk, O. Zinyemba, J. Darkwa, *Polyhedron* **2014**, *69*, 55 – 60.
[31] a) Y. Zhao, D. G. Truhlar, *Theor. Chem. Acc.* **2008**, *120*, 215 – 241; b) F. Weigend, R. Ahlrichs, *Phys. Chem. Chem. Phys.* **2005**, *7*, 3297 – 3305; c) A. Schäfer, C. Huber, R. Ahlrichs, *J. Chem. Phys.* **1994**, *100*, 5829; d) K. Eichkorn, F. Weigend, O. Treutler, R. Ahlrichs, *Theor. Chem. Acc.* **1997**, *97*, 119.
[32] Gaussian 16, M. J. Frisch, G. W. Trucks, H. B. Schlegel, G. E. Scuseria, M. A. Robb, J. R. Cheeseman, G. Scalmani, V. Barone, G. A. Peterson, H. Nakatsuji, X. Li, M. Caricato, A. V. Marenich, J. Bloino, B. G. Janesko, R. Gomperts, B. Mennucci, H. P. Hratchian, J. V. Ortiz, A. F. Izmaylov, J. L. Sonnenberg, D. Williams-Young, F. Ding, F. Lipparini, F. Egidi, J. Goings, B. Peng, A. Petrone, T. Henderson, D. Ranasinghe, V. G. Zakrzewski, J. Gao, N. Rega, G. Zheng, W. Liang, M. Hada, K. Ehara, K. Toyota, R. Fukuda, J. Hasegawa, M. Ishida, T. Nakajima, Y. Honda, O. Kitao, H. Nakai, T. Vreven, K. Throssell, J. A. Montgomery, Jr., J. E. Peralta, F. Ogliaro, M. J. Bearpark, J. J. Heyd, E. N. Brothers, K. N. Kudin, V. N. Staroverov, T. A. Keith, R. Robayashi, J. Normand, K. Raghavachari, A. P. Rendell, J. C. Burant, S. S. Iyengar, J. Tomasi, M. Ciossi, J. M. Millam, M. Klene, C. Adamo, R. Cammi, J. W. Ochterski, R. L. Martin, K. Morokuma, O. Farkas, J. B. Foresman, D. J. Fox, Gaussian Inc., Wallingford CT, **2016**.
[33] a) E. D. Glendening, C. R. Landis, F. Weinhold, *J. Comput. Chem.* **2013**, *34*, 1429 – 1437; b) E. D. Glendening, J. K. Badenhoop, A. E. Reed, J. E. Carpenter, J. A. Bohmann, C. M. Morales, C. R. Landis, F. Weinhold, *NBO 6.0*, Theoretical Chemistry Institute, University of Wisconsin, Madison, **2013**.
[34] Z. Otwinowski, W. Minor, *Methods Enzymol.* **1997**, *276*, 307 – 326.
[35] P. Coppens, in *Crystallographic Computing* (Eds.: F. R. Ahmed, S. R. Hall, C. P. Huber), Copenhagen, Munksgaard, **1970**, pp. 255 – 270.
[36] A. Altomare, G. Cascarano, C. Giacovazzo, A. Guagliardi, *J. Appl. Crystallogr.* **1994**, *27*, 1045 – 1050.

Manuscript received: August 28, 2019
Accepted manuscript online: October 6, 2019
Version of record online: November 15, 2019

